Gluon-initiated associated production boosts Higgs physics

Christoph Englert,[1,*] Matthew McCullough,[2,†] and Michael Spannowsky[3,‡]

[1]*SUPA, School of Physics and Astronomy, University of Glasgow, Glasgow G12 8QQ, United Kingdom*
[2]*Center for Theoretical Physics, Massachusetts Institute of Technology, Cambridge MA 02139, USA*
[3]*Institute for Particle Physics Phenomenology, Department of Physics, Durham University,*
DH1 3LE Durham, United Kingdom

Analyses of boosted Higgs bosons from associated production comprise some of the main search channels for the Higgs boson at the LHC. The gluon-initiated $gg \to hZ$ subprocess has largely been ignored in phenomenological analyses of boosted associated production although this contribution is sizable as the p_T spectrum for this process is maximized in the boosted regime due to the top quark loop threshold. In this paper, we discuss this contribution to boosted $pp \to hZ$ analyses in detail. We find there are previously overlooked modifications of standard model Higgs rates at the LHC which depend on the p_T cuts applied and can be significant. There are also important consequences for physics beyond the standard model as the $gg \to hZ$ process introduces significant dependence on the magnitude and sign of the Higgs-top quark coupling c_t, which is overlooked if it is assumed that associated production depends only on the Higgs-Z boson coupling as c_V^2. This new dependence on c_t impacts interpretations of Higgs rates in the contexts of supersymmetry, two Higgs doublet models, and general scenarios with modified couplings. We suggest that these effects be included in current and future LHC boosted Higgs analyses.

I. INTRODUCTION

The discovery of a boson at the LHC [1,2] largely consistent with the particle resulting from the standard model (SM) Higgs mechanism [3] marks the beginning of a new era of particle physics. For the first time we are provided with an opportunity to gain a better understanding of the electroweak scale through precise analyses and measurements of this newly discovered state. Crucial to the Higgs agenda is the precise measurement of the Higgs boson couplings to SM fields. The observed mass $m_h \simeq$ 125 GeV provides us with the fortunate circumstance that all dominant fermionic and bosonic Higgs decay channels are accessible at the LHC, and it is possible to probe the nature of the Higgs boson at $\lesssim 10\%$ precision at high luminosity [4].

The measurement of the Higgs-bottom quark coupling is enabled by exploiting boosted final states in conjunction with recently developed subjet technology [5] in associated production $pp \to hZ$. The latter is dominated by quark-initiated subprocesses, but there is also a large gluon-initiated contribution, $gg \to hZ$ [6,7], which has typically not been included in detail in the corresponding analyses.[1] The naïve cross section suppression of the gluon-initiated

subprocesses compared to the quark-initiated processes by roughly an order of magnitude [8] is not only compensated in part by much larger QCD perturbative corrections which enhance the role of the gluon-initiated component [9], but the top quark loop also induces a scale when absorptive parts of the scattering amplitude open up for invariant masses of the hZ system $m_{hZ} \gtrsim 2m_t$. It is straightforward to see that this phase-space region is characterized by boosted kinematics $p_{T,h} \gtrsim 150$ GeV. Hence, there is major sensitivity to $gg \to hZ$ in boosted analyses as these effects combine to lift the naïve cross section suppression of $gg \to hZ$. Because the gluon-initiated subprocess provides a nonnegligible contribution to the boosted $pp \to hZ$ rate at the LHC additional sensitivity to new physics is introduced with this process [10], and there is a significant impact on future Higgs coupling extractions at high LHC luminosities through the introduction of significant dependence on the magnitude and sign of the Higgs-top quark coupling. Furthermore, the gluon-initiated component is absent for $pp \to hW$. Hence, although the Higgs couplings to Z and W bosons may respect custodial symmetry to a high degree, i.e. $c_Z = c_W = c_V$, the gluon-initiated contribution means that $pp \to hZ$ and $pp \to hW$ need not respect this symmetry.[2] This subtlety is missed if only the $q\bar{q} \to hZ$, hW process is assumed in Higgs coupling fits. Gluon-initiated associated production also introduces sensitivity to new colored states coupled to the Higgs which enter the $gg \to hZ$ loops.

---

[*]christoph.englert@glasgow.ac.uk
[†]mccull@mit.edu
[‡]michael.spannowsky@durham.ac.uk
[1]The $gg \to hZ$ contribution can easily be missed by adopting an $\mathcal{O}(\alpha_s^2)$ K-factor normalization of a matched $q\bar{q} \to hZ$ sample. This does not reflect the differences in the differential characteristics of the gg and $q\bar{q}$ contributions, particularly with regard to the p_T spectrum.

---

[2]Throughout we define the Higgs coupling factors c_i as the ratio of the Higgs coupling to some SM state to the SM value.

We will first review $pp \to hZ$ production to make this work self-contained and subsequently perform a hadron-level analysis of the final state, including a leading order $gg \to hZ$ sample keeping all mass and Higgs coupling dependencies. We discuss the impact of including the effects of the $gg \to hZ$ process for SM Higgs rates at the LHC in boosted channels, finding that an accurate estimation of the cross section in boosted channels requires consideration of the full p_T distribution of the gluon-initiated contribution, rather than including this process as a rescaling of the quark-initiated distribution.[3] We also provide fits of the dependence of the associated production cross section on the Higgs couplings before and after typical selection cuts, including those relevant to $h \to \bar{b}b$ searches. We use this coupling dependence to evaluate the impact of the $gg \to hZ$ process on the extraction of new physics signatures from Higgs coupling fits.

II. GLUON-INITIATED *HZ* PRODUCTION IN THE BOOSTED REGIME

Given the importance of associated Higgs boson production, the gluon-initiated contribution to hZ production was calculated some time ago [6,7]. The QCD corrections to this process, however, have been made available only recently [9] in the $m_t \to \infty$, $m_b \to 0$ approximation. While the quark-initiated subprocesses follow a Drell-Yan-type paradigm with a moderate (next-to-)next-to leading order K-factor of $K \simeq 1.2$ the gluon-initiated contribution receives next-to-leading order (NLO) radiative corrections of $K \simeq 2$, similar to $gg \to h$, hh production [11,12], as a consequence of larger initial state color charge $C_A/C_F = 9/4$. We will not delve into the details of perturbative corrections, but will assume the total correction factor as reported in [8,9] as flat in the actual analysis. The characteristic leading order (LO) features, which are central to the discussion in this paper will also persist beyond LO.

Gluon-initiated associated production is computed from the Feynman topologies depicted in Fig. 1. The special role of the top quark follows from the threshold behavior of the amplitude which has a branch cut $s \geq 4m_t^2$, giving rise to an absorptive part of the amplitude related to other physical process according to the Cutkosky rules [13]. This can be seen in Fig. 2, where we compare the different contributions to $pp \to hZ$ at the LHC for $\sqrt{s} = 14$ TeV (see Fig. 3 for 7 TeV and 8 TeV results).[4] While this may be considered common knowledge, it is granted little attention in the estimation of Higgs signal rates and the coupling extraction effort. This is understandable in the light of the limited LHC Run I data which relies on total signal counts and
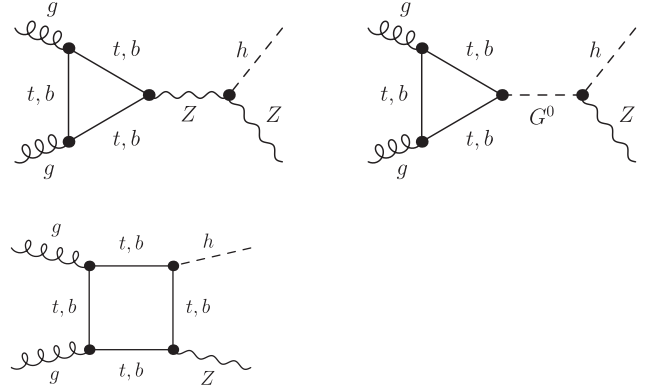
---

[3]Even when the event sample is corrected to distributions obtained with parton-level Monte Carlos the different shower profile of the gluon contribution is not included.

[4]We have cross-checked these results against existing calculations in the literature [6–9,14,15] and find excellent agreement.


FIG. 1. Feynman diagram topologies contributing to $gg \to hZ$ at leading order in general gauge.

hence the high $p_{T,h}$ analysis currently has a negligible impact on Higgs coupling extractions. However, this situation will change fundamentally with 14 TeV data and the high $p_{T,h}$ analyses will be central to the Higgs coupling extraction at a high luminosity run which will crucially rely on exclusive selections and differential Higgs cross sections.

We calculate the quark-initiated and one loop gluon-initiated associated production amplitudes using the FEYNARTS/FORMCALC/LOOPTOOLS [16] frameworks. We use a Monte Carlo calculation based on the Vbfnlo [17] framework to generate parton-level events in the Les Houches standard [18] which we pass to HERWIG++ [19] for showering and hadronization.

We apply typical hZ final state selection cuts by requiring exactly 2 oppositely charged same-flavor leptons satisfying $|\eta_l| < 2.5$ and $p_{T,l} > 30$ GeV and with invariant mass in the region $80 < m(l_1, l_2) < 100$ GeV. We tag boosted Z-boson candidates by requiring $p_T(l_1 + l_2) > 200$ GeV. To reconstruct the Higgs boson in $h \to \bar{b}b$ we combine jets using the Cambridge-Aachen algorithm with radius $R = 1.2$ and require a boosted Higgs boson candidate by requiring the jet p_T satisfies $p_{T,j} > 200$ GeV. At least one fat jet is required with $|\eta_j| < 2.5$ and the b-tagging is applied to this jet.

Jet substructure techniques are implemented as in the Butterworth-Davison-Rubin-Salam (BDRS) analysis [5] with a double b-tag on the filtered subjets. The doubly-tagged reconstructed Higgs jet has to have mass in the window $115\text{GeV} < m(\bar{b}b) < 135$ GeV. We impose a 60% signal tagging efficiency and a 2% fake tagging rate.

After the analysis steps described above we find a signal cross section of $\sigma = 0.2$ fb which contains the contribution from the gluon-initiated sample. We also include the relevant K factors as described earlier. The differential composition before cuts is shown in Fig. 2 and after cuts and BDRS analysis is shown in Fig. 4.

Obviously the boosted selection cuts (which cannot be relaxed unless the $t\bar{t}$ backgrounds are suppressed by other means) remove the m_t threshold behavior encountered in the gg subprocesses. Nonetheless the contribution is still
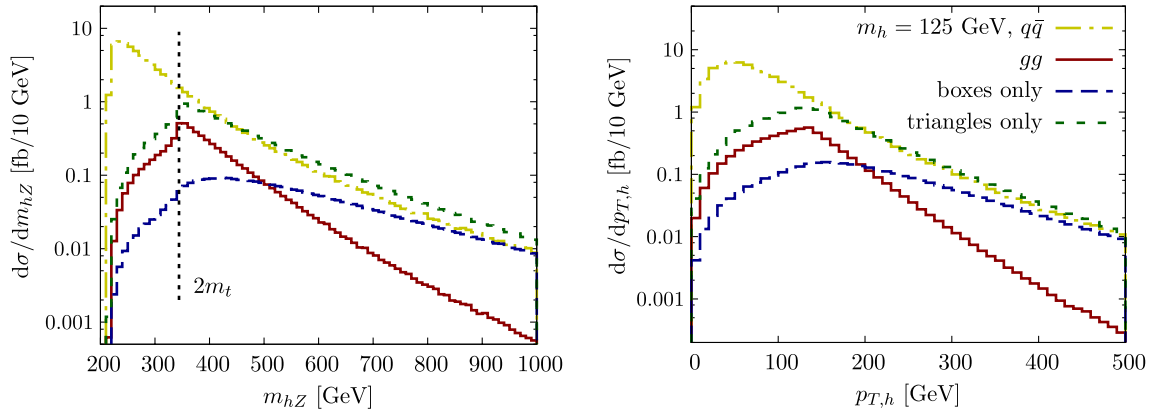
FIG. 2 (color online). Invariant hZ mass m_{hZ} (left) and p_T spectra (right) for $pp \to hZ$ production at $\sqrt{s} = 14$ TeV. The gluon-initiated and quark-initiated contributions are shown for comparison We also plot contributions from box and triangle diagrams to demonstrate the cancellation between the two in the sum.
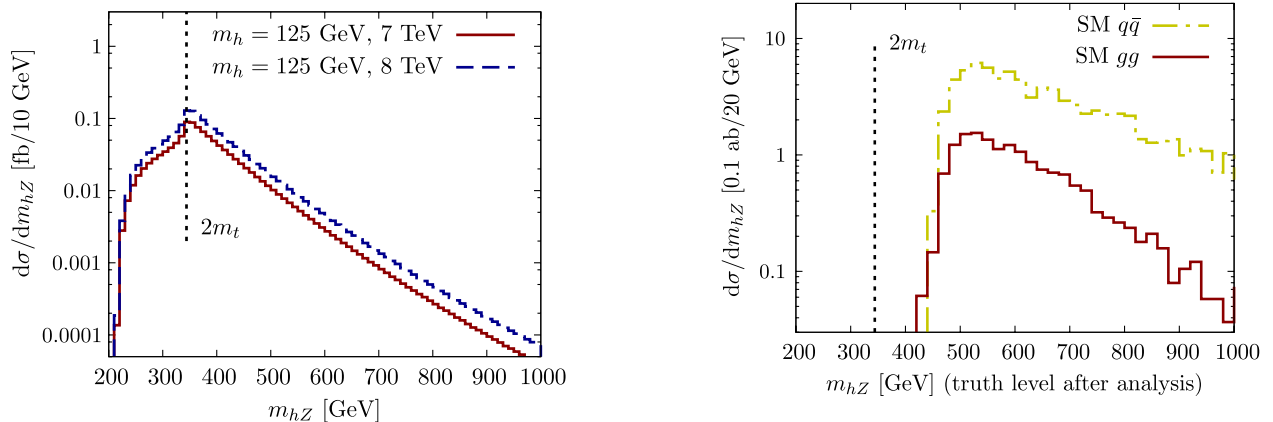

FIG. 3 (color online). Invariant hZ mass m_{hZ} for the gluon-initiated component of $pp \to hZ$ production at $\sqrt{s} = 7$ TeV and $\sqrt{s} = 8$ TeV for comparison with Fig. 2.

FIG. 4 (color online). Invariant truth-level hZ mass for $pp \to (h \to \bar{b}b)(Z \to \mu^+\mu^-, e^+e^-)$ production in the SM at $\sqrt{s} = 14$ TeV. These results are a direct reflection of Fig. 2 after the analysis cuts and the reconstruction have been applied. NLO correction factors as reported in Refs. [8,9] have been included to reflect the proper signal composition.

nonnegligible and the interplay of the box and triangle contributions can be used to formulate constraints on the involved couplings at large LHC luminosity.

III. IMPLICATIONS FOR SM RATES AT THE LHC

This result has implications for the extraction of SM Higgs rates in the boosted $pp \to hZ$, $h \to \bar{b}b$ channel. Currently rates are calculated in this channel by applying the selection cuts for boosted associated production to p_T distributions calculated at NLO which only include the quark-initiated component. Next-to-next-to-leading order (NNLO) corrections are taken into account by simply applying an overall rescaling to the distributions with the required K-factors, ensuring that the total associated production cross section matches the NNLO results. Gluon-initiated hZ is technically NNLO, hence the current methods overlook the differences in distributions between quark-initiated and gluon-initiated processes. These differences are significant, as demonstrated
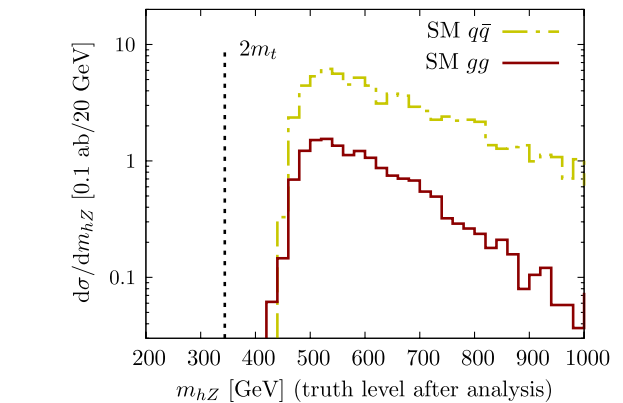
in Fig. 2. The gluon-initiated hZ distributions at 7 and 8 TeV are also shown and exhibit the same qualitative behavior.

Schematically, if we denote the application of typical selection cuts on an hZ production process at the LHC as $\mathrm{C}[\sigma]$ and the BDRS analysis on the $\bar{b}b$ final state as $\mathrm{B}[\sigma]$, then with current methods employed at the LHC the boosted associated production cross section after selection cuts is calculated as

$$\sigma_{\mathrm{Cuts}} = K^{\mathrm{eff}} \times \mathrm{C}[\sigma_{\bar{q}q}(pp \to hZ)], \qquad (1)$$

where the subscript $\bar{q}q$ denotes the quark-initiated process with distributions calculated at NLO.[5] After applying the full BDRS analysis the resulting cross section is

---

[5]Both QCD and EW corrections are included at NLO, however, NNLO effects, including gluon-initiated associated production, are only applied at the inclusive, or total cross section, level.

$$\sigma_{\text{BDRS}} = K^{\text{eff}} \times \text{B}[\text{C}[\sigma_{\bar{q}q}(pp \to hZ, h \to \bar{b}b)]]. \quad (2)$$

The effective K-factor is calculated from the inclusive cross sections as

$$K_{\text{eff}} = \frac{K^{\text{NNLO}}_{\bar{q}q} \times \sigma^{\text{Inc}}_{\bar{q}q} + K^{\text{NLO}}_{gg} \times \sigma^{\text{Inc}}_{gg}}{\sigma^{\text{LO,Inc}}_{\bar{q}q}}, \quad (3)$$

where the superscript "Inc" represents the fact that these quantities are calculated at the inclusive level. However, because the differential distributions for the boosted quark-initiated and gluon-initiated contributions are different they behave differently under the selection cuts and BDRS analysis, invalidating the approach sketched above. To obtain a more accurate result the cuts and BDRS analysis should be applied to events originating from both production mechanisms. Doing this one would calculate

$$\begin{aligned}\tilde{\sigma}_{\text{Cuts}} = {} & K^{\text{NNLO}}_{\bar{q}q} \times \text{C}[\sigma_{\bar{q}q}(pp \to hZ)] \\ & + K^{\text{NLO}}_{gg} \times \text{C}[\sigma_{gg}(pp \to hZ)], \quad (4)\end{aligned}$$

for the boosted cross section and

$$\begin{aligned}\tilde{\sigma}_{\text{BDRS}} = {} & K^{\text{NNLO}}_{\bar{q}q} \times \text{B}[\text{C}[\sigma_{\bar{q}q}(pp \to hZ, h \to \bar{b}b)]] \\ & + K^{\text{NLO}}_{gg} \times \text{B}[\text{C}[\sigma_{gg}(pp \to hZ, h \to \bar{b}b)]], \quad (5)\end{aligned}$$

for the cross section after applying the BDRS analysis.

Comparing the two methods we find $\tilde{\sigma}_{\text{Cuts}}/\sigma_{\text{Cuts}} \approx 1.09$, constituting a ~9% enhancement to the total Higgs associated production cross section after applying a typical set of cuts for boosted Higgs production at the LHC.[6] This arises as a greater fraction of the gluon-initiated events survive the selection cuts than for quark-initiated events, which can be understood from the p_T distribution in Fig. 2 where, for a p_T cut at 200 GeV, a greater fraction of the total gluon-initiated events will remain than for the quark-initiated events simply because the gluon-initiated distribution is peaked at greater p_T than the quark-initiated distribution.

For the BDRS analysis we find $\tilde{\sigma}_{\text{BDRS}}/\sigma_{\text{BDRS}} \approx 0.99$ showing that the previous effect is almost completely offset because a smaller fraction of gluon-initiated events survive the BDRS analysis than with Drell-Yan-initiated events. This offset is, however, dependent on the cuts and analysis applied so the effects of including the gluon-initiated contribution must be calculated for each independent analysis.

These numbers deserve some additional comments, since the interpretation of Eq. (3) is not entirely straightforward. The K^{eff} reweighting does not include the different gluon acceptance, hence leads to an increased cross section after cuts. Once the differential acceptance is included, Fig. 4, this artificial enhancement becomes weaker.

The theory uncertainties on the total associated production cross section at the LHC are ~5.4% [9], hence if one applies only the boosted selection cuts this previously unconsidered effect shifts the total cross section by almost 2σ relative to the assumed theory errors, however the shift is negligible if the BDRS analysis is also applied although this is an accidental cancellation and is not guaranteed to persist for different energies, selection cuts, or subjet methods. Thus to reduce theoretical uncertainty in signal estimation at the LHC it is clearly important to include distributions for both quark-initiated and gluon-initiated associated Higgs production, particularly in the boosted regime.

IV. IMPLICATIONS FOR NEW PHYSICS

It is clear that gluon-initiated associated production contributes significantly to associated production in the boosted regime. Within the SM this is of interest, however there are important consequences for searches for new physics in the Higgs sector. New physics can potentially modify associated Higgs production at the LHC [10,20]. The quark-initiated amplitude may be altered at LO through modified Higgs couplings or at NLO through the influence of new particles in loops [21]. Similarly the gluon-initiated $gg \to hZ$ amplitude may also be altered either through modified Higgs couplings to SM states, through the influence of new heavy colored states in loops, or new s-channel pseudoscalars [10]. Possibilities and scenarios for new states in the gluon-initiated amplitude are multifarious and a complete study is beyond the scope of this work hence we will only consider the case of modified Higgs couplings in detail.[7]

There has been a great deal of attention devoted to searching for new physics in the Higgs sector by modifying the electroweak couplings away from their SM values

$$g_i \to g_i(1 + \delta_i) = g_i c_i \quad (6)$$

either in an uncorrelated way [22], or by including the correlations present in some models such as 2HDMs [23], and fitting to the observed Higgs data.

---

[6]Specifically, for the quark-initiated contribution we have calculated the p_T distribution at LO, rather than NLO, however, due to the factorization of the dominant QCD correction, this has no impact on the comparison between gluon-initiated and quark-initiated distributions, which is the focus of this work.

[7]It would be interesting to calculate the effects of composite fermionic top partners as they would not only lead to additional corrections at the inclusive level but would also introduce new mass-thresholds into the p_T distribution with interesting implications for different p_T cuts. It has been shown that loops of supersymmetric stops do not modify the gluon-initiated associated production cross section [7].

Notwithstanding the theoretical shortcomings of such parameter rescalings related to gauge invariance, unitarity, and renormalizability, this procedure is often effective in constraining the effects of UV complete models. Ambiguities arise at NLO with Higgs coupling parameter rescalings due to the necessity of counterterms, whose structure is intimately related to the underlying gauge invariance of the electroweak sector. However, these issues can be avoided if only LO processes are considered in simple hypothesis tests to establish constraints. Fortunately, although the $gg \to hZ$ amplitude arises at one loop, and is technically a NNLO correction to associated production, this is a finite LO effect and the parameter rescaling procedure can be treated in exactly the manner as for the $gg \to h$ and $h \to \gamma\gamma$ amplitudes.

Studying Fig. 1 it is clear that the $gg \to hZ$ amplitude is sensitive to the hZZ, $h\bar{b}b$, and $h\bar{t}t$ couplings. Also, in many UV complete scenarios with modified hZZ couplings, such as 2HDMs, gauge invariance dictates that the hG^0Z couplings are modified by the same factor as the hZZ coupling, however the Goldstone couplings to G^0VV and $G^0\bar{f}f$ remain as in the SM, hence we choose this as our convention for Goldstone couplings.

Before moving on to a quantitative analysis it is worth pausing to consider the qualitative consequences for new physics encountered when including gluon-initiated events in boosted Higgs analyses. To the authors knowledge, thus far all of the many and varied studies of Higgs couplings in new physics scenarios have assumed that all of the signal in the boosted associated production channels arises from the quark-initiated process

$$\sigma(pp \to hZ) \sim \sigma(\bar{q}q \to hZ) \propto c_V^2 \qquad (7)$$

where the integration over parton distribution functions and the usual cuts appropriate to the boosted regime are implied. However, from this analysis it is clear that, due to the nonnegligible gluon-initiated contribution, in reality we have

$$\sigma(pp \to hZ) \sim a_{\bar{q}q}\sigma(\bar{q}q \to hZ) + a_{gg}\sigma(gg \to hZ) \quad (8)$$

$$\propto b_{\bar{q}q}c_V^2 + b_{gg}f(c_V, c_t) \qquad (9)$$

where the a's and b's are constants and we have not included dependence on c_b as the bottom-loop contributions are negligible. While this distinction may initially seem innocuous, it is important for constraining new physics with Higgs coupling fits to data.

Trivially one can see from Fig. 1 that due to the gluon-initiated contribution then, contrary to naïve expectations, even if $c_V = 0$ signal will still arise in boosted associated production channels due to the top-loop contribution.

Another interesting consequence is that the gluon-initiated contribution is sensitive to the sign of c_t due to interference between the triangles and boxes. This provides an additional handle on the sign of c_t complementary to the $h \to \gamma\gamma$ amplitude which is also sensitive to the sign. Additionally, in many modified Higgs sectors, such as 2HDMs, $c_V \leq 1$, which is intimately related to vector-boson scattering unitarity through sum rules [24]. Thus only assuming tree-level processes in the boosted associated production channels, as in Eq. (7), unavoidably leads to the artificial restriction $\sigma(pp \to hZ) \leq \sigma(pp \to hZ)_{SM}$ underlying any coupling fit. However, in many modified Higgs sectors, including again 2HDMs, it is quite common to have $c_t \geq 1$ and, by also including the gluon-initiated contribution, then for certain parameter regions this also allows $\sigma(pp \to hZ) \geq \sigma(pp \to hZ)_{SM}$, circumventing the artificially imposed restriction $\sigma(pp \to hZ) \leq \sigma(pp \to hZ)_{SM}$. Finally, based on precision electroweak measurements the assumption of custodial symmetry $c_Z = c_W = c_V$ is very robust. Assuming only quark-initiated associated production then leads to the assumption that the associated production processes $pp \to hZ$ and $pp \to hW$ also obey the same symmetry. However, if the coupling dependence of the gluon-initiated component is included in $pp \to hZ$ then the coupling dependence of $pp \to hZ$ and $pp \to hW$ does not exhibit custodial symmetry as the gluon-initiated component is absent for $pp \to hW$.

A. Inclusive associated production

Before turning to the case of boosted associated production, which is relevant in searches for $h \to \bar{b}b$, we will first consider the gluon-initiated contribution to the total associated production cross section. This regime is relevant in searches for $pp \to hZ$ where BDRS cuts are not applied, for example in the ATLAS [25] and CMS [26] searches for $pp \to hV$, $h \to WW^*$. From Fig. 1 we see that the gluon-initiated cross section must be a quadratic polynomial in c_V, c_t, and c_b. The parameter dependence of this contribution can be determined with a hadron-level calculation for six different parameter points. Including the K-factors and omitting the negligible dependence on c_b we find for $\sqrt{s} = 14$ TeV

$$\sigma_{gg}(pp \to hZ) = 136 - 133\delta_t + 61\delta_t^2 - 256\delta_t\delta_V$$
$$+ 406\delta_V - 332\delta_V^2 \text{ fb}. \qquad (10)$$

The usual quark-initiated contribution is

$$\sigma_{\bar{q}q}(pp \to hZ) = 847(1 + \delta_V)^2 \text{ fb}. \qquad (11)$$

Combining both results gives the parameter dependence of the total associated production cross section. The SM limit agrees with the results of [9] due to the K-factors. Normalizing the total cross section to the SM value we have
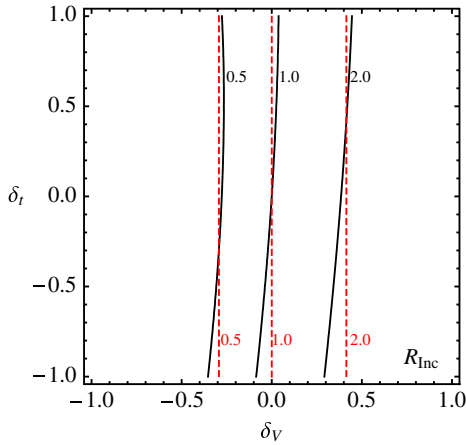
FIG. 5 (color online).   Parameter dependence of the inclusive associated production cross section relative to the SM result at 14 TeV after including K-factors and with the gluon-initiated contribution included (solid black) and omitted (dashed red). The result which omits the gluon-initiated contribution is a good approximation to the full result in this case.

$$R_{\text{Inc}} \equiv \frac{\sigma(pp \to hZ)}{\sigma(pp \to hZ)_{\text{SM}}}$$
$$= 1 - 0.14\delta_t + 0.06\delta_t^2 - 0.26\delta_t\delta_V + 2.14\delta_V + 1.20\delta_V^2.$$
$$(12)$$

Note that omitting the gluon-initiated component instead leads to $R_{\text{Inc}} = (1 + \delta_V)^2$ which, given the small coefficients of the δ_t components in Eq. (12) would appear a good approximation to the full result. This is demonstrated in Fig. 5 where we see that, due to the small overall contribution of the top quark loop, the dependence on δ_t is mild, and it is reasonable to assume in this case that the total associated production cross section is dominated by the quark-initiated process.

B. Boosted associated production

Now we apply the boosted selection cuts and BDRS analysis. We include K-factors and the gluon-initiated contribution and define the quantity R_{BDRS} which contains the full associated production cross section for $pp \to hZ$, $h \to \bar{b}b$ with selection cuts and BDRS analysis applied as a function of the relevant Higgs couplings. The coupling dependence which is due to the branching ratio for $h \to \bar{b}b$ is factored out in order to make explicit the coupling dependence of the production cross section in this channel, including the gluon-initiated process. Specifically, R_{BDRS} is defined as[8]

---

[8]Note that in Eq. (13) the branching ratio $\text{BR}^{h \to \bar{b}b}$ is included in the total cross section $\sigma(pp \to hZ, h \to \bar{b}b)$ hence R_{BDRS} gives the parameter dependence of the production cross section alone, as the parameter dependence of the branching ratio cancels out, by construction.

$$R_{\text{BDRS}} \equiv \frac{\sigma(pp \to hZ, h \to \bar{b}b)_{\text{BDRS}}}{\sigma(pp \to hZ, h \to \bar{b}b)_{\text{BDRS,SM}}} \frac{\text{BR}_{\text{SM}}^{h \to \bar{b}b}}{\text{BR}^{h \to \bar{b}b}} \quad (13)$$

and we find

$$R_{\text{BDRS}} = 1 - 0.42\delta_t + 0.50\delta_t^2 - 1.41\delta_t\delta_V + 2.41\delta_V$$
$$+ 1.90\delta_V^2. \quad (14)$$

Comparing Eq. (12) with Eq. (14) we see that in the boosted regime the dependence on δ_t is much stronger than for the inclusive cross section. The reason for this, alluded to earlier, is that in the boosted regime the requirement of larger p_T essentially means that the top quark loops are probed at CM energies close to, or in fact slightly larger than $2m_t$. Also, in the high p_T region the cancellation between box and triangle diagrams is much more delicate. Thus in the boosted regime the contribution from the top-quark loops is enhanced relative to their contribution in the inclusive rate.

It is illuminating to write Eq. (14) in terms of the rescaled couplings c_V and c_t

$$R_{\text{BDRS}} \approx 0.5c_t^2 - 1.4c_tc_V + 1.90c_V^2, \quad (15)$$

showing that at the SM point $c_V = c_t = 1$ there is a mild cancellation occurring between box and triangle diagrams. In beyond the standard model (BSM) scenarios with modified couplings this cancellation can be disrupted, further enhancing the role of the gluon-initiated process in boosted analyses.

In Fig. 6 we show the parameter dependence of of R_{BDRS} as defined in Eq. (13) at the 14 TeV LHC with K-factors and BDRS cuts imposed. As explained in the caption, Fig. 6 clearly demonstrates the necessity of including the gluon-initiated contribution in parameter fits involving associated production in the boosted regime at the LHC.

While the significance of the $h \to \bar{b}b$ signals from Run I of the LHC is relatively weak, Run II will lead to increased sensitivity in this channel and understanding signals or limits on new physics from the Run II Higgs search data will require interpreting the data in terms of well-motivated new physics models. There are many models one could consider, however we will only consider one particularly well-motivated model with interesting modifications to Higgs physics: the type II 2HDM. In addition to Higgs coupling modifications the additional heavy pseudoscalar field present in a 2HDM may also significantly modify the gluon-initiated associated production cross section through diagrams with an additional s-channel pseudoscalar [10]. To demonstrate the effects of the coupling modifications in the gluon-initiated process, rather than the role of new fields, we will assume that the pseudoscalar is decoupled and does not significantly affect rates. This is possible in a general 2HDM for arbitrary α and β parameters where there
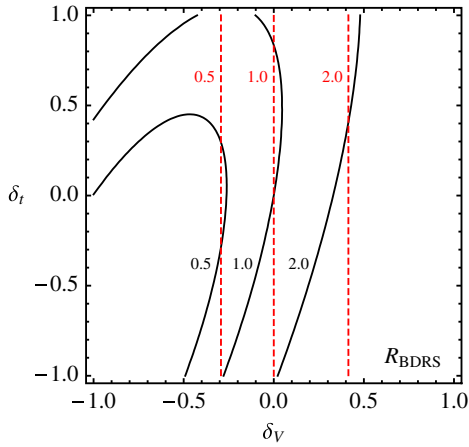
FIG. 6 (color online). Parameter dependence of R_{BDRS} as defined in Eq. (13) at 14 TeV after including K-factors and BDRS cuts with the gluon-initiated contribution included (solid black) and omitted (dashed red). This is a striking example of the importance of including the gluon-initiated process in parameter fits involving associated production at the LHC. For example, for the parameter point $\delta_V = 0$, ($c_V = 1$, $c_t = 0$), omitting the gluon-initiated process would lead to a purely SM-like cross section, whereas if it is included the cross section is almost doubled.

is the parameter freedom to take this limit, however the pseudoscalar may not be taken arbitrarily heavy in the MSSM, and we reserve study of this scenario to future work.

In Fig. 7 we show contours of the total $h \to \bar{b}b$ signal strength relative to the SM, denoted $\mu_{\bar{b}b}$, at the 14 TeV LHC without (above) and with (below) the effects of gluon-initiated processes included. It is immediately apparent that away from the decoupling limit ($\alpha = \beta - \pi/2$) the SM-like regions of parameter space are significantly different if gluon-initiated effects are included. Near the decoupling limit the inclusion of gluon-initiated effects leads to a significantly smaller region of parameter space with SM-like rates which would lead to significantly stronger constraints on 2HDM parameter space in the case of SM-like rate in the $h \to \bar{b}b$ channel during Run II of the LHC. We can study the approach to the decoupling limit by writing $\alpha - \beta = \delta - \pi/2$ and consider the parameter dependence of R_{BDRS}. Assuming we are close to the decoupling limit and expanding to first order in δ we find that with the gluon-initiated process omitted

$$\mu_{\bar{b}b}(\bar{q}q \to hZ) \approx 1 - \delta(0.2 \, \cot\beta + 0.7 \tan\beta), \quad (16)$$

whereas with the gluon-initiated process included

$$\mu_{\bar{b}b}(\bar{q}q, gg \to hZ) \approx 1 - \delta(0.6 \, \cot\beta + 0.7 \tan\beta), \quad (17)$$

and the dependence on deviations from the decoupling limit is much stronger at low $\tan\beta$. This is not surprising as the gluon-initiated associated production introduces strong
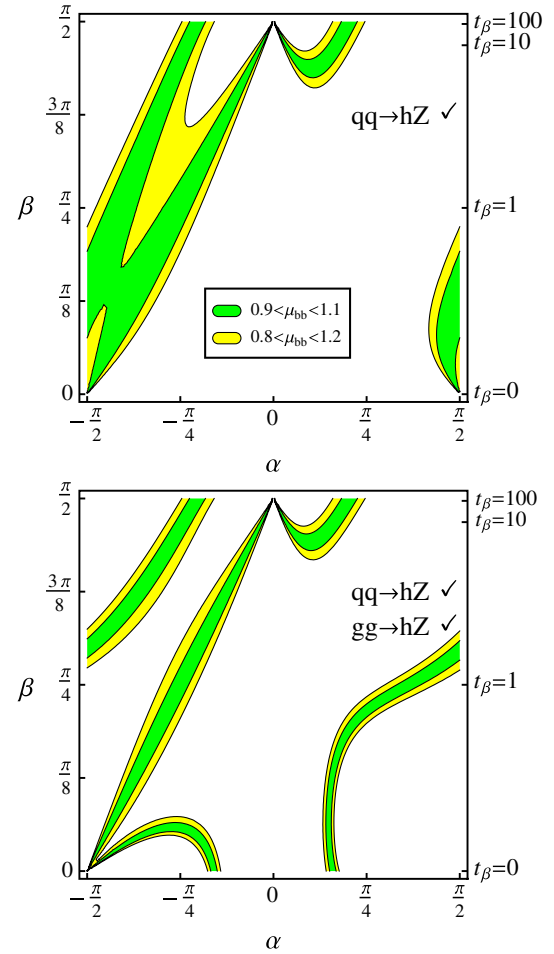

FIG. 7 (color online). Contours of the total signal strength relative to the SM in the $h \to \bar{b}b$ channel with BDRS analysis applied for a Type II 2HDM with the effects of gluon-initiated associated production omitted (above) and included (below). The heavy pseudoscalar is assumed to be decoupled, and not included in this calculation. In this calculation we have rescaled all couplings, but not included triangle diagrams with $gg \to A^* \to hZ$, which may become important if the additional pseudoscalar A is light. Including the gluon-initiated associated production effects leads to significant modifications of the total $h \to \bar{b}b$ rate at the LHC in the type II 2HDM. In particular, once these effects are included, deviations in the total rate are more rapid as one moves away from the decoupling limit $\alpha = \beta - \pi/2$. This is due to the rapid growth in the gluon-initiated cross section away from the SM Higgs couplings as the cancellation between boxes and triangles is spoiled.

dependence of the cross section on the Higgs-top quark coupling, which in this limit is given by $c_t \approx 1 + \delta \cot\beta$.

Looking away from the decoupling limit in Fig. 7 the inclusion of gluon-initiated associated production changes the parameter dependence of the signal rate, and hence must be included to properly investigate or constrain these regions of parameter space in boosted $h \to \bar{b}b$ searches.

We have only considered the impact of these new effects in one particular example, the type II 2HDM, however it is

clear that gluon-initiated associated production will be an important consideration in future efforts to evaluate the viability of many beyond the standard model scenarios, such as all varieties of 2HDM and many other interesting possibilities.

V. SUMMARY

The transition from the discovery to precision phase of Higgs boson physics at the LHC has begun. As it lies at the heart of hierarchy problem, there is great potential for the Higgs boson as a future harbinger of new physics. Maximizing this discovery potential will require greater precision and scrutiny of theoretical predictions, a fact which is well appreciated for SM calculations, but which is also applicable to BSM scenarios where leading-order calculations, which are the status quo, may fail to capture important effects. Leading-order assumptions in BSM Higgs physics may introduce the undesirable possibility of mischaracterizing, or missing altogether, signals of new physics: a point made clear in this work.

We have demonstrated that the p_T spectrum of the gluon-initiated contribution to associated production is fundamentally different to the dominant quark-initiated contribution. This is due to the threshold behavior of the top-loop at transverse momenta $p_T \sim m_t$. Although technically a NNLO contribution, it is important that the p_T dependence of the gluon-initiated component is included in the estimation of Higgs boson signals in the boosted regime, rather than using current methods which include this contribution at the inclusive level through an overall rescaling of the quark-initiated distribution, obfuscating the critical differences between these two different processes under p_T cuts and boosted analysis techniques.

This is relevant for SM Higgs boson searches in boosted channels.

Looking toward BSM Higgs scenarios the gluon-initiated component may introduce sensitivity to new colored states through loops which would have interesting threshold behavior at high p_T due to the mass of new states. This sensitivity is overlooked by making leading-order assumptions for associated production. Furthermore, we have explicitly demonstrated that the gluon-initiated contribution introduces dependence of the associated production cross section on the Higgs-top quark coupling c_t, especially in the boosted regime, and this dependence can become important away from the SM limit as a cancellation between triangle and box diagrams is spoiled, enhancing the effect. This new dependence on c_t has important consequences for models where the Higgs couplings are altered as in supersymmetry, 2HDMs, and many other scenarios. The correct interpretation of boosted Higgs signals at the LHC in the context of BSM scenarios, including general Higgs coupling fits, will require treatment of the gluon-initiated contribution to boosted associated production in addition to the quark-initiated Drell-Yan process.

ACKNOWLEDGMENTS

[1] S. Chatrchyan *et al.* (CMS Collaboration), Phys. Lett. B **716**, 30 (2012).

[2] G. Aad *et al.* (ATLAS Collaboration), Phys. Lett. B **716**, 1 (2012).

[3] F. Englert and R. Brout, Phys. Rev. Lett. **13**, 321 (1964); P. W. Higgs, Phys. Rev. Lett. **12**, 132 (1964); Phys. Rev. Lett. **13**, 508 (1964); G. S. Guralnik, C. R. Hagen, and T. W. B. Kibble, *ibid.* **13**, 585 (1964).

[4] T. Plehn and M. Rauch, Europhys. Lett. **100**, 11002 (2012).

[5] J. M. Butterworth, A. R. Davison, M. Rubin, and G. P. Salam, Phys. Rev. Lett. **100**, 242001 (2008); D. E. Soper and M. Spannowsky, J. High Energy Phys. 08 (**2010**) 029.

[6] D. A. Dicus and C. Kao, Phys. Rev. D **38**, 1008 (1988); Phys. Rev. D **42**, 2412(E) (1990); B. A. Kniehl, Phys. Rev. D **42**, 2253 (1990); Nucl. Phys. **B345**, 331 (1990).

[7] B. A. Kniehl and C. P. Palisoc, Phys. Rev. D **85**, 075027 (2012).

[8] R. Hamberg, W. L. van Neerven, and T. Matsuura, Nucl. Phys. **B359**, 343 (1991); Nucl. Phys. **B644**, 403(E) (2002); T. Han and S. Willenbrock, Phys. Lett. B **273**, 167 (1991); M. L. Ciccolini, S. Dittmaier, and M. Kramer, Phys. Rev. D **68**, 073003 (2003); O. Brein, A. Djouadi, and R. Harlander, Phys. Lett. B **579**, 149 (2004); G. Ferrera, M. Grazzini, and F. Tramontano, Phys. Rev. Lett. **107**, 152003 (2011); O. Brein, R. Harlander, M. Wiesemann, and T. Zirke, Eur. Phys. J. C **72**, 1868 (2012); A. Denner, S. Dittmaier, S. Kallweit, and A. Muck, J. High Energy Phys. 03 (**2012**) 075; A. Banfi and J. Cancino, Phys. Lett. B **718**, 499 (2012); S. Dawson, T. Han, W. K. Lai, A. K. Leibovich, and I. Lewis, Phys. Rev. D **86**, 074007 (2012); O. Brein, R. V. Harlander, and T. J. E. Zirke, Comput. Phys. Commun. **184**, 998 (2013).

[9] L. Altenkamp, S. Dittmaier, R. V. Harlander, H. Rzehak, and T. J. E. Zirke, J. High Energy Phys. 02 (**2013**) 078.

[10] R. V. Harlander, S. Liebler, and T. Zirke, arXiv:1307.8122.

[11] D. Graudenz, M. Spira, and P. M. Zerwas, Phys. Rev. Lett. **70,** 1372 (1993); M. Spira, A. Djouadi, D. Graudenz, and P. M. Zerwas, Nucl. Phys. **B453,** 17 (1995).

[12] S. Dawson, S. Dittmaier, and M. Spira, Phys. Rev. D **58,** 115012 (1998).

[13] R. E. Cutkosky, J. Math. Phys. (N.Y.) **1,** 429 (1960).

[14] T. Gleisberg, S. Hoeche, F. Krauss, M. Schonherr, S. Schumann, F. Siegert, and J. Winter, J. High Energy Phys. 02 (**2009**) 007.

[15] J. Alwall, P. Demin, S. de Visscher, R. Frederix, M. Herquet, F. Maltoni, T. Plehn, D. L. Rainwater, and T. Stelzer, J. High Energy Phys. 09 (**2007**) 028.

[16] T. Hahn, Comput. Phys. Commun. **140,** 418 (2001); T. Hahn and M. Perez-Victoria, Comput. Phys. Commun. **118,** 153 (1999).

[17] K. Arnold, M. Bahr, G. Bozzi, F. Campanario, C. Englert, T. Figy, N. Greiner, and C. Hackstein *et al.*, Comput. Phys. Commun. **180,** 1661 (2009).

[18] E. Boos, M. Dobbs, W. Giele, I. Hinchliffe, J. Huston, V. Ilyin, J. Kanzaki, and K. Kato *et al.*, hep-ph/0109068.

[19] M. Bahr *et al.*, Eur. Phys. J. C **58,** 639 (2008).

[20] K. Nishiwaki, S. Niyogi, and A. Shivaji, arXiv:1309.6907.

[21] C. Englert and M. McCullough, J. High Energy Phys. 07 (**2013**) 168.

[22] D. Carmi, A. Falkowski, E. Kuflik, and T. Volansky, J. High Energy Phys. 07 (**2012**) 136; A. Azatov, R. Contino, and J. Galloway, J. High Energy Phys. 04 (**2012**) 127; A. Azatov, R. Contino, and J. Galloway, J. High Energy Phys. 04 (**2013**) 140(E); J. R. Espinosa, C. Grojean, M. Mühlleitner, and M. Trott, J. High Energy Phys. 05 (**2012**) 097; M. Klute, R. Lafaye, T. Plehn, M. Rauch, and D. Zerwas, Phys. Rev. Lett. **109,** 101801 (2012); T. Corbett, O. J. P. Eboli, J. Gonzalez-Fraile, and M. C. Gonzalez-Garcia, Phys. Rev. D **86,** 075013 (2012); J. R. Espinosa, C. Grojean, M. Mühlleitner, and M. Trott, J. High Energy Phys. 12 (**2012**) 045; D. Carmi, A. Falkowski, E. Kuflik, T. Volansky, and J. Zupan, J. High Energy Phys. 10 (**2012**) 196; T. Plehn and M. Rauch, Europhys. Lett. **100,** 11002 (2012);

T. Corbett, O. J. P. Eboli, J. Gonzalez-Fraile, and M. C. Gonzalez-Garcia, Phys. Rev. D **87,** 015022 (2013).

[23] A. Celis, V. Ilisie, and A. Pich, J. High Energy Phys. 07 (**2013**) 053; D. Lopez-Val, T. Plehn, and M. Rauch, J. High Energy Phys. 10 (**2013**) 134; K. Cheung, J. S. Lee, and P.-Y. Tseng, arXiv:1310.3937.

[24] J. F. Gunion, H. E. Haber, and J. Wudka, Phys. Rev. D **43,** 904 (1991).

[25] ATLAS Collaboration, Report No. ATLAS-CONF-2013-075 (unpublished).

[26] CMS Collaboration, Report No. CMS-PAS-HIG-13-017 (unpublished).